0013-7227/07/$15.00/0
Printed in U.S.A.

Endocrinology 148(11):5248–5257

doi: 10.1210/en.2007-0265

Fish Glucose Transporter (GLUT)-4 Differs from Rat GLUT4 in Its Traffic Characteristics but Can Translocate to the Cell Surface in Response to Insulin in Skeletal Muscle Cells

Mònica Díaz,* Costin N. Antonescu,* Encarnación Capilla, Amira Klip, and Josep V. Planas

Departament de Fisiologia (M.D., J.V.P.), Facultat de Biologia, Universitat de Barcelona, 08028 Barcelona, Spain; Programme in Cell Biology (C.N.A., A.K.), The Hospital for Sick Children, Toronto, Ontario, Canada M5G 1X8; and Department of Pharmacological Sciences (E.C.), Stony Brook University, Stony Brook, New York 11794-8651

In mammals, glucose transporter (GLUT)-4 plays an important role in glucose homeostasis mediating insulin action to increase glucose uptake in insulin-responsive tissues. In the basal state, GLUT4 is located in intracellular compartments and upon insulin stimulation is recruited to the plasma membrane, allowing glucose entry into the cell. Compared with mammals, fish are less efficient restoring plasma glucose after dietary or exogenous glucose administration. Recently our group cloned a GLUT4-homolog in skeletal muscle from brown trout (btGLUT4) that differs in protein motifs believed to be important for endocytosis and sorting of mammalian GLUT4. To study the traffic of btGLUT4, we generated a stable L6 muscle cell line overexpressing *myc*-tagged btGLUT4 (btGLUT4*myc*). Insulin stimulated btGLUT4*myc* recruitment to the cell surface, although to a lesser extent than rat-GLUT4*myc*, and enhanced glucose uptake. Interestingly, btGLUT4*myc* showed a higher steady-state level at the cell surface under basal conditions than rat-GLUT4*myc* due to a higher rate of recycling of btGLUT4*myc* and not to a slower endocytic rate, compared with rat-GLUT4*myc*. Furthermore, unlike rat-GLUT4*myc*, btGLUT4*myc* had a diffuse distribution throughout the cytoplasm of L6 myoblasts. In primary brown trout skeletal muscle cells, insulin also promoted the translocation of endogenous btGLUT4 to the plasma membrane and enhanced glucose transport. Moreover, btGLUT4 exhibited a diffuse intracellular localization in unstimulated trout myocytes. Our data suggest that btGLUT4 is subjected to a different intracellular traffic from rat-GLUT4 and may explain the relative glucose intolerance observed in fish. (*Endocrinology* 148: 5248–5257, 2007)

IN MAMMALS, GLUCOSE TRANSPORTER (GLUT)-4 is the main glucose transporter expressed in insulin-sensitive tissues such as adipose tissue, skeletal muscle, and heart (1). This facilitative glucose transporter exerts its function at the plasma membrane allowing the entry of glucose into muscle and fat cells. It has been demonstrated that in the basal state, most of the amount of GLUT4 is located in intracellular stores and that in response to insulin is rapidly translocated to the cell surface resulting in an increase in cellular glucose transport (2, 3). For this reason GLUT4 has been described as the insulin-responsive glucose transporter and is important for the rapid glucose disposal from blood in a situation of increased plasma glucose levels, such as during the postprandial period.

In our efforts to understand the role of GLUT4 in fish carbohydrate metabolism and its regulation by insulin, our group has identified, for the first time in nonmammalian vertebrates, two GLUT4-homologs in fish, one in brown trout skeletal muscle (btGLUT4) and another one in salmon adipose tissue (okGLUT4) (4, 5). Kinetic studies of okGLUT4 expressed in *Xenopus* oocytes have shown that it is a selective glucose transporter but with lower affinity than mammalian GLUT4 (4). This difference in affinity may explain the well-known lower ability of fish to clear a glucose load, when compared with mammals (6, 7). However, additional properties of the transporter traffic may contribute to this effect. We have shown that insulin is able to cause the translocation of okGLUT4 to the plasma membrane when transiently expressed in 3T3-L1 adipocytes, a response that may underlie the effect of insulin enhancing glucose uptake in isolated trout adipocytes (4).

In fish, skeletal muscle is the major site for glucose uptake because it represents more than 50% of the body weight (6). Unfortunately, the role of insulin on glucose transport in fish skeletal muscle is poorly understood. We previously demonstrated that blood insulin levels may regulate btGLUT4 expression in skeletal muscle (8, 9), probably by a direct action of insulin on trout skeletal muscle cells regulating the expression of the btGLUT4 gene (Díaz, M., and J. Planas, unpublished observations). However, we do not know whether btGLUT4 traffic in muscle cells is regulated by insulin. To characterize the regulation of btGLUT4 transloca-

First Published Online August 16, 2007

* M.D. and C.N.A. contributed equally to this work.

Abbreviations: btGLUT4, GLUT4-homolog in brown trout skeletal muscle; btGLUT4*myc*, overexpressing *myc*-tagged btGLUT4; 2-DG, 2-deoxy-D-[2,6-^{3}H]glucose; FBS, fetal bovine serum; GLUT, glucose transporter; GS, goat serum; GSC, GLUT4 storage compartment; HA, hemagglutinin; HES, buffer of HEPES, sucrose, dithiothreitol, magnesium acetate, potassium acetate, and zinc chloride; HRP, horseradish peroxidase; okGLUT4, GLUT4-homolog in salmon adipose tissue; OPD, *o*-phenylenediamide; PFA, paraformaldehyde; PM, plasma membrane; TGN, trans-Golgi network.

***Endocrinology* is published monthly by The Endocrine Society (http://www.endo-society.org), the foremost professional society serving the endocrine community.**

tion in muscle cells and directly compare it with that of the mammalian GLUT4, we generated an L6 cell line that stably overexpresses btGLUT4 harboring an exofacial *myc* epitope (btGLUT4*myc*). These cells are thus a useful comparative to the well-characterized L6 cell line stably expressing rat-GLUT4myc (10, 11). Our results indicate that btGLUT4*myc* translocates to the cell surface of L6 cells in response to insulin but that its steady-state level at the cell surface under basal conditions is higher, compared with rat-GLUT4*myc*. This difference is caused by a faster externalization rate and not by a slower endocytic rate of btGLUT4*myc*. In addition, the intracellular distribution of btGLUT4*myc* in L6 myoblasts as well as endogenous btGLUT4 in trout muscle cells is diffuse throughout the cytoplasm and not concentrated in the perinuclear region. We suggest that the difference in traffic between fish and mammalian GLUT4 could be related to differences in the sequence of certain protein motifs that may result in a different interaction between fish GLUT4 and GLUT4-interacting proteins. Therefore, understanding the traffic characteristics of fish GLUT4, which could be considered a natural mutant of mammalian GLUT4, could be important for unraveling the mechanisms responsible for the intracellular retention of GLUT4 in mammalian cells.

Materials and Methods

Materials

α-MEM and fetal bovine serum (FBS) were from Invitrogen (Prat del Llobregat, Spain). DMEM and all other tissue culture reagents were purchased from Sigma (Tres Cantos, Madrid, Spain). Plasticware for cell culture was from BD Biosciences (Madrid, Spain). The Effectene transfection reagent was from QIAGEN (Hilden, Germany). Human insulin (Humulin R) was from Lilly (Alcobendas, Madrid, Spain). Salmon insulin was kindly supplied by Dr. E. M. Plisetskaya (University of Washington, Seattle, WA). Cationic silica was a kind gift of Dr. David E. James (Garvan Institute of Medical Research, Sydney, Australia). Indinavir was kindly provided by Merck (Haarlem, The Netherlands). Monoclonal and polyclonal anti-*myc* antibodies were purchased from Santa Cruz Biotechnology (Santa Cruz, CA). Polyclonal anti-GLUT1 antibody was obtained from Abcam (Cambridge, UK) and kindly donated by Dr. Antonio Zorzano (Universitat de Barcelona, Barcelona, Spain). Horseradish peroxidase (HRP)-conjugated goat antirabbit IgG was from Jackson ImmunoResearch (Soham, UK). AlexaFluor488-conjugated goat antirabbit IgG was obtained from Invitrogen. Immunofluore mounting medium was from ICN Biochemicals (Madrid, Spain). 2-Deoxy-D-[2,6-^{3}H]glucose (2-DG) was purchased from Amersham Biosciences (Barcelona, Spain). Bio-Rad protein assay was obtained from Bio-Rad (Prat del Llobregat, Spain).

Construction of c-myc epitope-tagged btGLUT4 cDNA expression vector

The cDNA sequence of human c-*myc* epitope (5′-GCAGAGGAGCAAAAGCTTATTTCTGAAGAGGACTTGCTTAAG-3′) was introduced into the cDNA coding sequence of btGLUT4 (AF247395) (5), between Gly^{58} and Glu^{59}, in the region corresponding to the first extracellular loop of btGLUT4 protein. This insertion was carried out by the overlapping PCR method. Two rounds of PCR were necessary to obtain the final construct. In the first round, two DNA fragments were obtained separately: one fragment corresponding to the btGLUT4 cDNA sequence coding for the amino acids 1–58 and carrying the cDNA sequence of c-*myc* epitope at the 3′ end and another DNA fragment corresponding to the btGLUT4 cDNA sequence coding for the amino acids 59–503 and carrying the c-*myc* sequence at the 5′ end. At the second round of PCR, these two initial fragments were used as templates to obtain the cDNA coding sequence of btGLUT4 with the inserted *myc* sequence (btGLUT4*myc*). Finally btGLUT4*myc* was subcloned into the mammalian expression vector pCXN2 (12).

Generation of L6-btGLUT4myc stable cell line

Parental L6 myoblasts were cotransfected with the expression vector pCXN2-btGLUT4*myc* and the pSV2-bsr plasmid (a blasticidin S deaminase expression plasmid) using the Effectene transfection reagent (QIAGEN). Transfected cells were selected with blasticidin S hydrochloride. Fifteen clones were isolated and their btGLUT4*myc* expression was analyzed by immunoprecipitation and subsequent immunoblotting against the *myc* epitope. The ability of each clone to fuse and form myotubes was also monitored.

L6 cell culture

L6 myoblasts were maintained with α-MEM containing 10% FBS and 1% antibiotic-antimycotic solution (10,000 U/ml penicillin G, 10 mg/ml streptomycin, 25 μg/ml amphotericin B) in an atmosphere of 5% CO_2 at 37 C. For GLUT4*myc*-expressing L6 cells, the medium was also supplemented with 2 μg/ml blasticidin hydrochloride. To induce differentiation of myoblasts into myotubes, the percentage of FBS in the medium was reduced to 2%.

Isolation of muscle cells from brown trout (Salmo trutta)

Brown trout of 5–10 g body weight were obtained from the Piscifactoria de Bagà (Barcelona, Spain) and were maintained in the facilities of the Faculty of Biology at the University of Barcelona in a closed-water flow circuit with water at a temperature of 12 C. Animals (40–80 for each isolation) were killed by a blow to the head and immersed in 70% ethanol for 30 sec to sterilize external surfaces. Muscle cells were isolated and cultured following a protocol described by Castillo *et al.* (13) and Fauconneau and Paboeuf (14). Cells were cultured on six-well plates for plasma membrane preparation or 12-well plates for glucose uptake assay at a density of $3–4 \times 10^6$ and 1×10^6 cells/well, respectively. Plates were previously treated with poly-L-lysine and laminin to facilitate muscle cell adhesion. After 24 h of plating, plates were washed to eliminate nonadherent cells to the well. Cells were maintained at 18 C with DMEM containing 9 mM $NaHCO_3$, 20 mM HEPES, 10% FBS and antibiotic-antimycotic cocktail (100 U/ml penicillin, 100 μg/ml streptomycin, 250 ng/ml amphotericin B). All cultures were monitored by observation under an inverted microscope. The experimental protocols used for trout in this study have been reviewed and approved by the Ethics and Animal Welfare Committee of the University of Barcelona, Spain.

Determination of the proportion of GLUT4myc at the cell surface

L6 myoblasts were serum deprived for 3–5 h and subsequently stimulated, or not, with 100 nM insulin for 20 min. Medium was then removed by repeated washing in ice-cold PBS (154 mM NaCl, 5.6 mM Na_2HPO_4, 1.1 mM KH_2PO_4) supplemented with 1 mM $CaCl_2$ and 1 mM $MgCl_2$ at 4 C [PBS+ (pH 7.4)]. To label cell surface GLUT4*myc* in intact L6 myoblasts, cells were blocked in 5% goat serum (GS) in PBS+ for 15 min and then incubated with α-*myc* antibody solution (1.0 μg/ml in PBS+ with 5% GS) for 1 h at 4 C. After labeling, excess α-*myc* antibodies were removed by extensive washing in ice-cold PBS+. Cells were then fixed in 4% paraformaldehyde (PFA) in PBS+ for 30 min and quenched in 100 mM glycine in PBS+ for 10 min, all at 4 C. To label total cellular GLUT4*myc*, a separate set of L6 cells were first fixed in 4% PFA in PBS+ for 30 min, quenched in 100 mM glycine in PBS+ for 10 min, and then permeabilized in 0.1% Triton X-100 for 30 min, all at 4 C. After blocking in 5% GS in PBS+ for 15 min, total cellular GLUT4 was labeled by incubation with α-*myc* antibody solution (1.0 μg/ml in PBS+ with 5% GS) for 1 h at 4 C, after which excess antibodies were removed by extensive washing in ice-cold PBS+. Both cell surface or total cellular GLUT4-bound anti-*myc* antibodies were probed by HRP-conjugated secondary antibodies followed by detection of bound HRP by *o*-phenylenediamide (OPD) assay, as previously described (15). The fraction of GLUT4*myc* at the cell surface, measured in triplicate, was taken as the ratio of surface GLUT4*myc* to total cellular GLUT4*myc*.

Glucose uptake measurements

Determination of 2-DG uptake in L6 cells was performed as described by Huang *et al.* (16) with some modifications. Glucose uptake was

assessed for 5 min in HEPES-buffered saline [140 mM NaCl, 20 mM HEPES, 5 mM KCl, 2.5 mM $MgSO_4$, 1 mM $CaCl_2$ (pH 7.4)] containing 10 μM 2-DG (0.5 μCi/ml 2-[^{3}H]DG) at room temperature. Subsequently, cells were rinsed three times with an ice-cold solution containing 0.9% NaCl and 20 mM D-glucose. To quantify the radioactivity incorporated by the cell, cells were lysed with 0.05 N NaOH, and lysates were counted with scintillation liquid in a β-counter. Nonspecific uptake was carried out in the presence of cytochalasin B (20–50 μM) during the assay, and these values were subtracted from all other values. Total protein content was measured with the Bio-Rad protein assay.

In trout muscle cells, glucose uptake assay was performed as follows. After 5 d in culture, trout muscle cells were serum starved for 4 h and subsequently incubated in the absence or presence of 1 μM salmon insulin for 30 min at 18 C. Cells were washed twice with PBS and incubated with HEPES-buffered saline containing 50 μM 2-DG (2 μCi/ml 2-[^{3}H]DG) for 30 min at 18 C. After this period, transport solution was removed and cells were rinsed three times with ice-cold PBS containing 50 mM glucose. Finally, cells were lysed with 0.1 N NaOH and 0.1% sodium dodecyl sulfate, and radioactivity was determined by scintillation counting. Protein concentration was measured with the Bio-Rad protein assay. Nonspecific uptake was carried out in the presence of 10 μM cytochalasin B in the transport solution, and these values were subtracted of all other values.

GLUT4myc internalization assay

L6 myoblasts were serum deprived for 3–5 h and then washed in ice-cold PBS+. To label cell surface GLUT4*myc* in intact L6 myoblasts, cells were blocked in 5% GS in PBS+ for 15 min and then incubated with α-*myc* antibody solution (1.0 μg/ml in PBS+ with 5% GS) for 1 h at 4 C. The cells were then washed extensively in ice-cold PBS+, twice in 37 C PBS+ (rewarming stage), and subsequently returned to 37 C α-MEM for 0, 2, 5, or 10 min, as indicated (internalization stage). After internalization of surface proteins, L6 cells were rapidly washed in ice-cold PBS+ to arrest membrane traffic, fixed in 4% PFA in PBS+ for 10 min, and quenched by 100 mM glycine in PBS+ for 10 min, all at 4 C. GLUT4-bound anti-*myc* antibodies remaining at the cell surface were probed by HRP-conjugated secondary antibodies followed by detection of bound HRP by OPD assay, as previously described (15). The amount of GLUT4*myc* remaining at the cell surface after various times of internalization, measured in triplicate, was expressed as the fraction of GLUT4 at the cell surface before internalization.

GLUT4myc recycling assay

L6 myoblasts were serum deprived for 3 h and then incubated with 1.0 μg/ml α-*myc* antibody (in α-MEM) for 50, 100, 200, 300, or 400 min at 37 C to label the GLUT4 recycling through the plasma membrane (PM) during the indicated time. Subsequently, L6 myoblasts were extensively washed in ice-cold PBS+ to remove excess antibodies and then fixed in 4% PFA in PBS+ for 30 min and quenched in 100 mM glycine in PBS+ for 10 min, all at 4 C. After blocking in 5% GS in PBS+ for 15 min, GLUT4-bound anti-*myc* antibodies were probed by HRP-conjugated secondary antibodies followed by detection of bound HRP by OPD assay, as previously described (15). The total cellular amount of GLUT4*myc* was determined in permeabilized cells as described above. The amount of GLUT4*myc* having recycled through the PM, measured in triplicate, was expressed as a ratio of total cellular GLUT4*myc*.

Immunofluorescence microscopy

Twenty-four hours after seeding on glass coverslips, L6 myoblasts stably expressing either fish- or rat-GLUT4*myc* (15) were transfected by Lipofectamine 2000 (Invitrogen, Carlsbad, CA), as described by the manufacturer, with cDNA encoding hemagglutinin (HA) epitope-tagged rat-GLUT4 (rat-GLUT4-HA). Twenty-four hours after transfection, L6 myoblasts were serum deprived for 3–5 h, washed extensively with ice-cold PBS+, fixed for 30 min in 4% PFA in PBS+, quenched in 100 mM glycine in PBS+ for 10 min, and then permeabilized in 0.1% Triton X-100 in PBS+ for 30 min, all at 4 C. L6 myoblasts were then blocked in 5% GS for 15 min and incubated with both polyclonal α-*myc* and monoclonal α-HA antibodies for 1 h at 4 C. For colocalization studies of GLUT4*myc* and GLUT1, L6 myoblasts were incubated with a monoclonal anti-*myc* antibody and a polyclonal antibody against the C terminus of GLUT1. After removal of excess antibodies by extensive washing in ice-cold PBS+, cells were incubated with appropriate fluorophore-conjugated secondary antibodies. After removal of excess secondary antibodies by washing in PBS+, coverslips were then mounted in Dako on glass slides.

To perform immunofluorescence analysis in brown trout muscle cells, these were grown on glass coverslips previously coated with poly-L-lysine and laminin. Cells were rinsed with PBS and fixed with 3% PFA in PBS for 15 min at room temperature. After washing three times, cells were sequentially incubated with 100 mM glycine in PBS for 10 min and permeabilized with 0.1% saponin in PBS for 20 min. All the subsequent incubations and washes were made in the presence of 0.1% saponin. Cells were blocked with 10% GS for 20 min and subsequently incubated with the primary antibody against okGLUT4 (4) diluted 1:50 in blocking solution for 1 h at room temperature. After several washes with 0.1% saponin in PBS, cells were incubated with AlexaFluor488-conjugated secondary antibody for 1 h at room temperature. Coverslips were washed and mounted with Immunofluore mounting medium. Confocal images were obtained with a SPII laser confocal fluorescence microscope (Leica, Heidelberg, Germany) with a ×63 objective.

Plasma membrane isolation

Plasma membrane preparations were obtained as described by Chaney and Jacobson (17) and Larance *et al.* (18). Trout muscle cells at d 5 of culture were serum deprived for 4 h and incubated in the absence or presence of 1 μM salmon insulin at 18 C for 30 min. After washing the cells with ice-cold PBS, cells were rinsed twice with ice-cold coating buffer [20 mM MES, 150 mM NaCl, 280 mM sorbitol (pH 5.0–5.5)] and cationic silica 1% in coating buffer was added to the cells for 2 min at 4 C. The excess of silica was removed and cells were washed with ice-cold coating buffer. After incubation with 1 mg/ml polyacrylic acid for 2 min at 4 C, cells were washed with coating buffer and lysed with modified HES buffer [20 mM HEPES, 250 mM sucrose, 1 mM dithiothreitol, 1 mM magnesium acetate, 100 mM potassium acetate, 0.5 mM zinc chloride (pH 7.4)]. The lysate was passed 12 times through a 22-gauge needle and 6 times through a 27-gauge needle. One volume of nycodenz (100% in modified HES buffer) was added to the lysate that was layered onto 0.5 ml 70% nycodenz and centrifuged in a swing-out rotor at 41,545 × *g* for 20 min at 4 C. The pellet was resuspended in modified HES buffer and spun at 500 × *g* for 5 min at 4 C three times to remove all nycodenz. The final pellet was resuspended in Laemmli sample buffer, heated at 65 C for 10 min, and centrifuged at 10,000 × *g* for 5 min. The resulting supernatant was stored at −80 C until immunoblot analysis.

Electrophoresis and immunoblotting

Plasma membrane samples (4 μg protein) were subjected to 12% SDS-PAGE and proteins were transferred to a polyvinylidene difluoride membrane. The membrane was blocked with blocking buffer (Tris-buffered saline containing 0.1% Tween 20 and 5% nonfat dry milk) for 2 h and subsequently incubated overnight with a polyclonal anti-okGLUT4 antibody diluted to 1:500 in blocking buffer at 4 C. After several washes, the membrane was incubated with HRP-conjugated secondary antibody for 1 h at room temperature. Immunoreactive bands were visualized by chemiluminescence and quantified with an image analyzer (version 1.11; TotalLab, Nonlinear Dynamics, Newcastle upon Tyne, UK).

Statistical analysis

Values are given as mean ± SE. Analysis of statistical significance of differences in measurements between samples was done by one-way ANOVA with Newman-Keul's posttest and Student's *t* test.

Results

In the generation of the L6-btGLUT4*myc* cell line, 15 independent clones were isolated and evaluated according to the level of expression of btGLUT4*myc* and their ability to

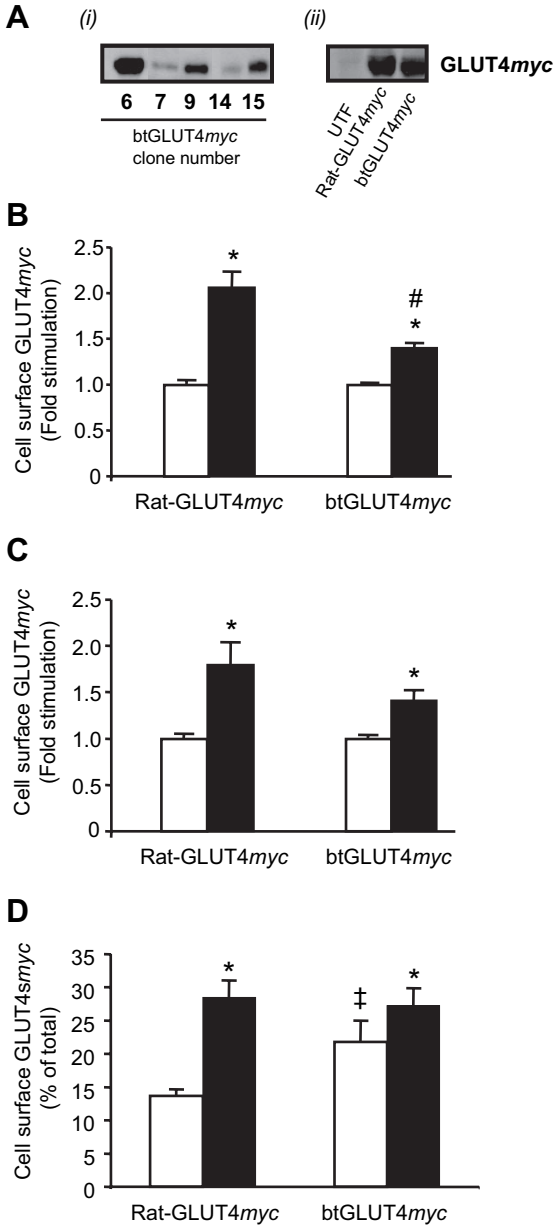

FIG. 1. Insulin enhances the presence of both btGLUT4*myc* and rat-GLUT4*myc* at the plasma membrane, although in the basal state a larger fraction of btGLUT4*myc* is already located at the cell surface. A, Expression levels of btGLUT4*myc* were analyzed in different isolated L6 clones (i) and compared with that of L6-ratGLUT4*myc* cells (ii). Total protein extracts from myoblasts of each cell line (300 μg), including the untransfected (UTF) wild-type cells, were immunoprecipitated using anti-*myc* monoclonal antibody. Immunocomplexes were resolved by 10% SDS-PAGE and analyzed by immunoblotting using a polyclonal antibody against the *myc* epitope. In all subsequent experiments, only clone 6 was used. Cell surface rat- and btGLUT4*myc* levels were measured in L6 myoblasts (B) and myotubes (C) in response to insulin. Rat- and btGLUT4*myc*-expressing cells were serum deprived for 3–5 h and subsequently incubated in the absence (*white bars*) or presence (*black bars*) of 100 nM insulin for 20 min at 37 C. After the incubation period, the cell surface level of GLUT4*myc* was determined as described in *Materials and Methods*. Results are expressed as fold stimulation above the basal level of each cell line, which was set to 1. Results shown are the means ± SE of three independent experiments, each performed in triplicate. D, The proportion of GLUT4*myc* at the cell surface, as a percentage of total cellular GLUT4*myc*, was determined in L6 myoblasts stably expressing either rat- or btGLUT4*my,* and stimulated (*black bars*) or not (*white bars*) with 100 nM insulin, as described in *Materials and Methods*. Results shown are the means ± SE of six independent experiments. *, $P < 0.05$, relative to respective basal condition; #, $P < 0.05$, relative to rat-GLUT4myc insulin condition; ‡, $P < 0.05$, relative to rat-GLUT4*myc* basal condition.

form myotubes. Only five clones showed a detectable expression of btGLUT4*myc* (Fig. 1Ai). Clone 6 exhibited the highest GLUT4*myc* expression that was similar to the expression of GLUT4*myc* in L6-ratGLUT4*myc* myoblasts (Fig. 1Aii). Clones 14 and 15 were discarded because of their slower growth. In all subsequent experiments, only the results for clone 6 are shown.

*btGLUT4*myc *translocates to the plasma membrane in response to insulin but shows a higher presence in the plasma membrane than rat-GLUT4myc in the absence of insulin*

The amount of GLUT4*myc* present at the cell surface was measured in L6 myoblasts that stably express btGLUT4*myc* and in those that express rat-GLUT4*myc* (15). Insulin caused an increase of GLUT4*myc* at the plasma membrane in L6-btGLUT4*myc* myoblasts as well as the L6-ratGLUT4*myc* myoblasts (Fig. 1B). The net gain of GLUT4*myc* at the cell surface in response to insulin was significantly ($P < 0.05$) higher in L6-ratGLUT4*myc* (2.05 ± 0.17) than in the L6-btGLUT4*myc* cells (1.39 ± 0.06). In myotubes, both rat- and btGLUT4*myc* levels at the plasma membrane increased after an insulin treatment in the same proportion as in myoblasts (Fig. 1C). Similar results were obtained with clones 7 and 9 at both myoblast and myotube stages (data not shown). Interestingly, when cell surface GLUT4*myc* is expressed as the percentage of total GLUT4*myc*, the amount of GLUT4*myc* at the plasma membrane under basal conditions was significantly higher for L6-btGLUT4*myc* cells (above 20% of the total amount of btGLUT4*myc*), compared with L6-ratGLUT4*myc* cells (Fig. 1D).

Insulin stimulates glucose uptake in L6-btGLUT4myc cells

Glucose uptake measurements in the L6-btGLUT4*myc* cell line were conducted to assess the effect of btGLUT4*myc* overexpression in L6 cells at the myoblast and myotube stages. After 3–5 h of serum starvation, cells were incubated with different concentrations of insulin (0, 10, and 100 nM) for 20 min followed by the glucose uptake assay. In parallel, the same experiments were also performed in wild-type L6 cells (untransfected cells) and L6-ratGLUT4*myc* cells. In myoblasts, L6-btGLUT4*myc* cells together with wild-type L6 cells and L6-ratGLUT4*myc* cells showed insulin-stimulated glucose uptake (Fig. 2). In all three cell lines, insulin already increased glucose uptake at 10 nM, and in wild-type and rat-GLUT4*myc*-expressing myoblasts, this stimulation was slightly higher at 100 nM. In myotubes, insulin also significantly stimulated glucose uptake in all three cell lines (data not shown). Similar results were obtained with clones 7 and 9 at both myoblast and myotube stages (data not shown). L6-btGLUT4*myc* myoblasts exhibited a basal glucose uptake rate 2.1-fold higher than that of wild-type cells (10.86 ±

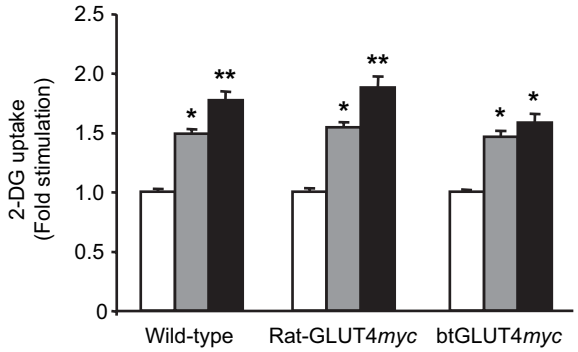

FIG. 2. Glucose uptake in L6-btGLUT4*myc* cells is insulin responsive. In L6 myoblasts, insulin stimulated 2-DG uptake. Cells were serum deprived for 3–5 h and subsequently incubated with 0 (*white bars*), 10 (*gray bars*), or 100 nM (*black bars*) insulin for 20 min at 37 C. After the incubation period, 2-DG uptake assay was performed as described in *Materials and Methods*. Results are expressed as fold stimulation above basal level of each cell line, which was set to 1. Results shown are the means ± SE of six independent experiments (except for wild-type cells that were four) each performed in triplicate. *, $P < 0.05$, relative to respective basal condition of each cell line; **, $P < 0.05$, relative to respective basal and 10 nM insulin conditions.

0.78 *vs.* 5.21 ± 0.67 pmol 2-DG mg^{-1}/min^{-1}, respectively), whereas the glucose uptake rate of L6-ratGLUT4*myc* myoblasts under basal conditions was 3.8-fold higher than that of L6 wild-type cells (19.83 ± 1.49 *vs.* 5.21 ± 0.67 pmol 2-DG mg^{-1}/min^{-1}, respectively). The lower basal glucose uptake rate of L6-btGLUT4*myc* myoblasts, compared with L6-ratGLUT4*myc* cells, could be attributed, in part, to the lower affinity for glucose described for fish GLUT4 (4) and/or possible differences in activity of the transporter because the expression levels of btGLUT4*myc* and rat-GLUT4*myc* in the L6 lines appear to be similar (Fig. 1Ai).

To determine whether the endofacial structure/conformation of fish GLUT4 is different from that of mammalian GLUT4, we used transport inhibitors known to bind GLUT4. We first investigated the sensitivity of L6-btGLUT4*myc* cell line to cytochalasin B, a well-known inhibitor of facilitated glucose transport, and compared it with the rat-GLUT4*myc* cell line (Fig. 3A). Glucose uptake was clearly inhibited by cytochalasin B in a concentration-dependent manner on both rat- and btGLUT4*myc* cells, but rat-GLUT4*myc* cells were more sensitive to the inhibitor. For example, 1 μM cytochalasin B reduced glucose uptake in L6-ratGLUT4*myc* myoblasts by 87%, whereas the same concentration of cytochalasin B reduced glucose uptake in L6-btGLUT4*myc* only to 50% of the initial glucose uptake. Second, we investigated the effects of indinavir, a known inhibitor of mammalian GLUT4, on glucose transport in L6-btGLUT4*myc* and L6-ratGLUT4*myc* myoblasts. In both cell lines, indinavir inhibited glucose uptake in a dose-dependent manner, but the inhibitor was more effective in L6-ratGLUT4*myc* than L6-btGLUT4*myc* cells at all concentrations tested (Fig. 3B). Therefore, these data support the hypothesis that the differences in the primary structure between fish and mammalian GLUT4 may affect their ability to bind GLUT4-interacting factors.

btGLUT4myc internalizes at a similar rate as rat-GLUT4myc but recycles faster

Given that the level of GLUT4 is the balance between the internalization and exocytic rates, we set out to investigate

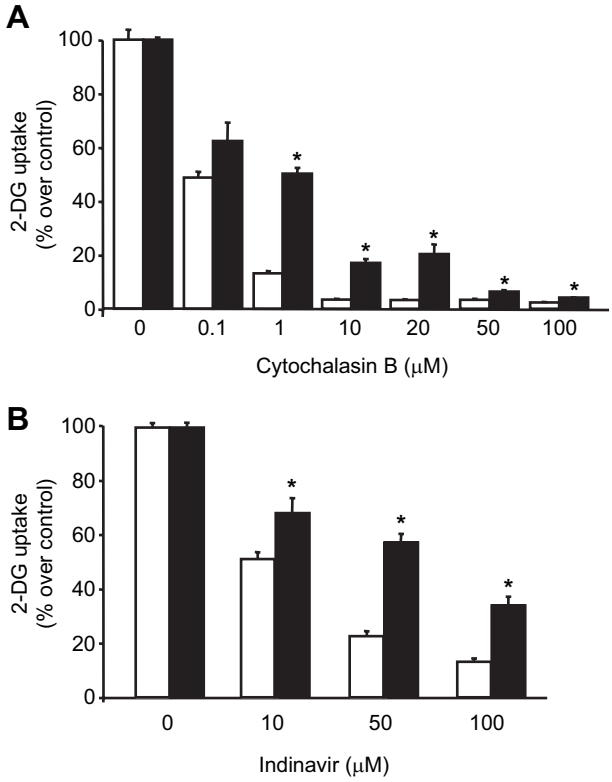

FIG. 3. Glucose uptake in L6-btGLUT4*myc* cells shows lower sensitivity to inhibitors than in L6-ratGLUT4*myc* cells. The inhibition of 2-DG uptake in L6-ratGLUT4*myc* (*white bars*) and L6-btGLUT4*myc* (*black bars*) myoblasts by cytochalasin B and indinavir is shown in A and B, respectively. 2-DG uptake assay was performed in the presence of the indicated concentrations of cytochalasin B or indinavir in the transport solution. Results are expressed as a percentage of uptake over the basal value obtained without inhibitor. Results shown are the means ± SE of three independent experiments each performed in triplicate. *, $P < 0.05$, relative to rat-GLUT4*myc* at the same concentration of inhibitor.

the possible cause for the higher basal level of btGLUT4*myc* at the plasma membrane. First, we analyzed the internalization of rat-GLUT4*myc* and btGLUT4*myc* by quantifying the amount of *myc*-tagged transporters remaining at the cell surface after 2, 5, and 10 min of endocytosis. Under basal conditions the percentage of GLUT4*myc* remaining at the plasma membrane was similar for btGLUT4*myc* and rat-GLUT4*myc* (Fig. 4A), suggesting that the internalization rate of btGLUT4*myc* is similar to that of rat-GLUT4*myc*. In view of these results, we next investigated whether recycling was different between trout and rat-GLUT4*myc*. Therefore, to determine the rate of appearance of btGLUT4*myc* at the cell surface, we incubated L6 myoblasts in α-MEM with anti-*myc* antibody during different times to label any GLUT4*myc* molecule arriving at the plasma membrane. After this period the amount of labeled GLUT4*myc* at the plasma membrane was quantified and referred to the total amount of GLUT4*myc*. At 200 and 300 min, a greater amount of btGLUT4*myc* had reached the cell surface, compared with rat-GLUT4*myc* (Fig. 4B). Therefore, these results suggest that btGLUT4 recycles faster through the plasma membrane than its mammalian counterpart.

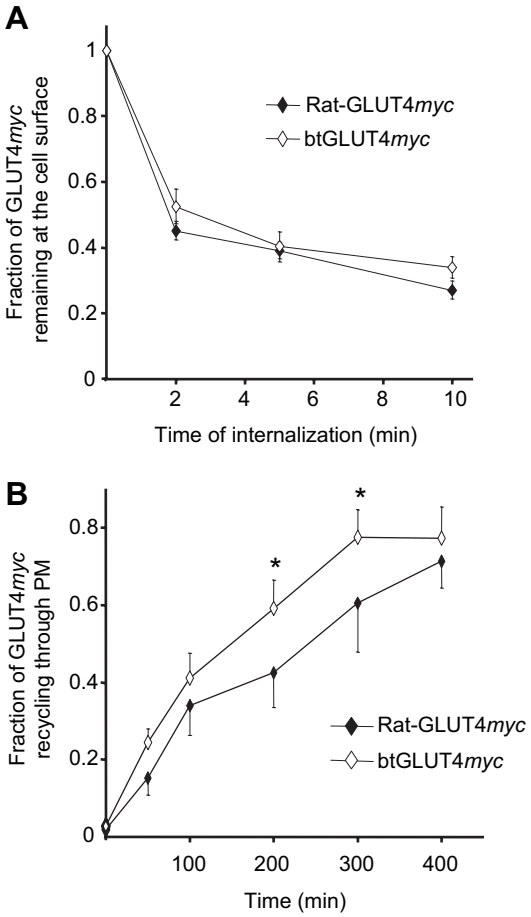

FIG. 4. btGLUT4*myc* is internalized at a similar rate than rat-GLUT4*myc* but recycles through the plasma membrane more quickly. A, The fraction of either rat- or btGLUT4*myc* remaining at the cell surface at various times was determined in L6 myoblasts as described in *Materials and Methods*. Results shown are the means ± SE of 15–29 independent experiments. B, The fraction of rat- or btGLUT4*myc* that recycles through the plasma membrane at various times was determined as described in *Materials and Methods*. Results shown are the means ± SE of seven independent experiments. *, $P < 0.01$, relative to fraction of rat-GLUT4*myc* recycled, at the indicated times.

btGLUT4myc differs from rat-GLUT4myc in its subcellular localization

Thus far, the increased levels of btGLUT4*myc* at the plasma membrane in the basal state coupled with the faster recycling of this transporter suggested that btGLUT4*myc* could have a different traffic route than rat-GLUT4*myc*. Therefore, we hypothesized that the subcellular distribution of btGLUT4*myc* might differ from that of rat-GLUT4*myc*. To address this issue, we transiently transfected btGLUT4*myc*- and rat-GLUT4*myc*-expressing myoblasts with the rat-GLUT4-HA cDNA. Immunofluorescence detection of *myc* and HA epitopes revealed that, in the same cell, btGLUT4*myc* had a more diffuse distribution throughout the cytoplasm than rat-GLUT4-HA, which was mainly concentrated at the perinuclear region (Fig. 5A, panels 1 and 2). On the other hand, both rat-GLUT4*myc* and rat-GLUT4-HA showed tight polarized perinuclear concentration when expressed in the same cell (Fig. 5A, panels 3 and 4). In contrast to rat-GLUT4*myc*, btGLUT4*myc* was detected in the cytoplasm (Fig. 5, A, panel 1, and B), similar to GLUT1 (which is vastly cytosolic) but also showed clear perinuclear localization, although to a lesser extent than rat-GLUT4*myc* (Fig. 5B). To confirm that the distribution of btGLUT4 observed in mammalian cells is also observed in fish cells, we investigated the subcellular localization of endogenous btGLUT4 by immu-

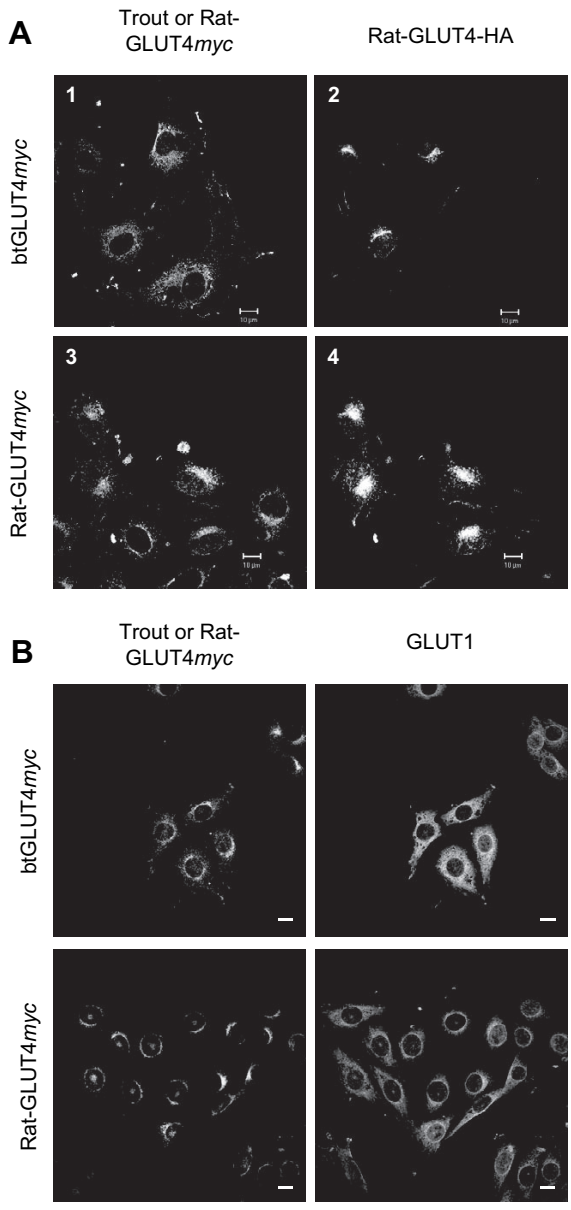

FIG. 5. btGLUT4 differs from rat-GLUT4 in its subcellular distribution. A, Immunolocalization studies of btGLUT4 and rat-GLUT4 in L6 myoblasts stably expressing rat- (panels 3 and 4) or btGLUT4*myc* (panels 1 and 2) transfected with rat-GLUT4-HA. The cellular localization of *myc*- (panels 1 and 3) or HA-tagged GLUT4 (panels 2 and 4) was determined as described in *Materials and Methods*. *Scale bars*, 10 μm. B, Immunofluorescence of GLUT4*myc* and GLUT1 in L6 myoblasts stably expressing rat- or btGLUT4*myc*. The cellular localization of GLUT1 or *myc*-tagged GLUT4 was determined as described in *Materials and Methods*. *Scale bars*, 20 μm. Shown are micrographs, representative of four independent experiments, showing a similar single optical z-section of the perinuclear region of either trout- or rat-GLUT4*myc*-L6 myoblasts obtained by confocal microscopy.

nofluorescence in a primary culture of trout muscle cells in the basal state. As shown in Fig. 6, btGLUT4 immunoreactivity was clearly distributed throughout the cytoplasm, but not predominantly in the perinuclear region, in both trout myoblasts and myotubes. Nevertheless, a slight accumulation of endogenous btGLUT4 around the nucleus was detected in trout myotubes. Furthermore, the labeling for btGLUT4 appeared more intense in fully differentiated myotubes than in myoblasts, which correlates with the increase in btGLUT4 mRNA expression observed during *in vitro* differentiation of trout muscle cells (Díaz, M., and J. Planas, unpublished observations).

Insulin increases the amount of btGLUT4 at the plasma membrane and glucose uptake in trout myocytes

Having demonstrated that insulin stimulates the translocation of btGLUT4*myc* when stably expressed in L6 cells, we set out to determine whether endogenous btGLUT4 is able to translocate to the cell surface upon insulin stimulation in fish muscle cells. To do this, we analyzed the amount of GLUT4 present in purified plasma membrane fractions from trout muscle cells previously incubated in the absence or presence of 1 μM insulin for 30 min by immunoblotting. Our results indicate that the content of endogenous btGLUT4 at the plasma membrane was significantly increased by insulin in trout muscle cells (Fig. 7A), providing the first evidence in nonmammalian vertebrates that endogenous GLUT4 translocates to the plasma membrane in response to insulin in muscle cells. Glucose uptake measurements in trout myocytes showed that insulin also stimulates glucose uptake, probably as a consequence of btGLUT4 translocation (Fig. 7B).

Discussion

In the present study, we investigated the traffic of btGLUT4, a GLUT4-homolog identified in brown trout skeletal muscle (5), and its regulation by insulin in muscle cells. Interestingly, btGLUT4 shows differences in protein motifs (*e.g.* ^{5}FQQI^{8}, ^{489}LL^{490}) believed to be important for endocytosis and sorting of mammalian GLUT4 (19–24). In view of this fact, we hypothesized that btGLUT4 could show differences in cellular traffic with respect to mammalian GLUT4 and that by understanding the nature of these differences, we would increase our knowledge on the mechanisms regulating GLUT4 traffic in mammalian cells.

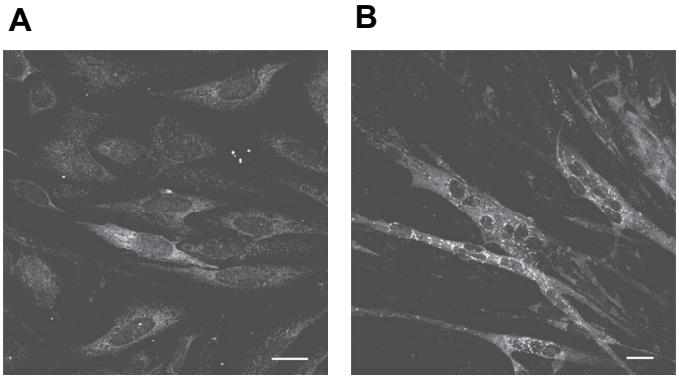

FIG. 6. btGLUT4 has a diffuse distribution throughout the cytoplasm in trout muscle cells. Immunolocalization of endogenous btGLUT4 was determined in unstimulated trout myoblasts (A) and myotubes (B), as described in *Materials and Methods*. Representative micrographs are shown. *Scale bars*, 20 μm.

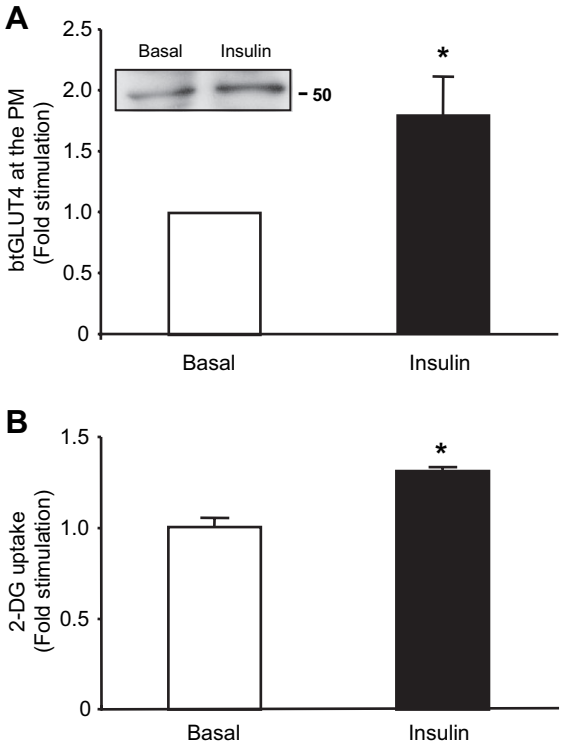

FIG. 7. Insulin stimulates the translocation of endogenous btGLUT4 and glucose uptake in trout primary myoblasts. A, The increase in the steady-state levels of endogenous btGLUT4 in the PM of trout muscle cells in response to insulin is shown. Trout myoblasts, after 5 d in primary culture, were serum starved for 4 h and subsequently incubated in the absence or presence of 1 μM insulin for 30 min at 18 C. After the incubation period, plasma membranes were obtained as described in *Materials and Methods*. Values are means ± SE from the densitometric analysis of four independent experiments and were set to 1 in the basal group. *Inset*, A representative btGLUT4 immunoblot is shown. B, The effects of insulin on 2-DG uptake are shown. After 5 d of culture trout myoblasts were serum starved for 4 h and subsequently incubated in the absence or presence of 1 μM insulin for 30 min at 18 C. After the incubation period, 2-DG uptake assay was performed as indicated in *Materials and Methods*. Results are expressed as fold stimulation above basal, which was set to 1. Values are the means ± SE from a representative experiment performed in triplicate. *, $P < 0.05$, relative to basal.

Steady-state distribution of btGLUT4

To carry out a direct comparison between the traffic of btGLUT4 and that of its rat homolog, we expressed both transporters in the same L6 cell background, a rat muscle cell line that has been well characterized in terms of insulin response and glucose transport regulation (10, 25–27). Generation of a stable L6 cell line expressing the *myc*-tagged rat-GLUT4 has provided a useful tool to study the intracellular traffic of GLUT4 and its regulation by insulin in mammalian skeletal muscle cells (10, 11, 15). Thus, we generated a stable L6 cell line overexpressing *myc*-tagged btGLUT4 (L6-btGLUT4*myc*). Tagging GLUT4 protein in an exofacial domain (loop between transmembrane domains 1 and 2)

with the *myc* epitope allows measuring the amount of transporter inserted at the plasma membrane in intact cells by an easy and highly sensitive method (15) and also allows discerning the endogenous GLUT4 from the exogenously expressed GLUT4. Steady-state levels of btGLUT4*myc* and rat-GLUT4*myc*, used as a control, at the cell surface were examined in response to insulin. Our results indicate that insulin stimulates the translocation of btGLUT4*myc* to the plasma membrane in a manner similar to rat-GLUT4*myc*, as previously described (16, 28). Furthermore, the increase in the amount of GLUT4*myc* at the cell surface in response to insulin led to an enhanced glucose uptake activity in L6-btGLUT4*myc* and L6-ratGLUT4*myc* cells at the myoblast and myotube stages. The observed effects of insulin increasing glucose uptake in L6-ratGLUT4*myc* cells agree with previous reports (11, 29).

To confirm that insulin-stimulated translocation of btGLUT4 occurs in fish cells, we investigated the effects of insulin on btGLUT4 translocation in primary brown trout skeletal muscle cells. Immunoblotting analysis of purified plasma membranes revealed that insulin increases the amount of endogenous GLUT4 at the plasma membrane of brown trout muscle cells, resulting in an improved ability of these cells to take up glucose as shown by the increase in the glucose uptake rate in insulin-treated cells. The stimulation of glucose transport by insulin in brown trout skeletal muscle cells is in agreement with previous studies using primary cultures of muscle satellite cells from rainbow trout (30), chicken (31), sheep (32), and humans (33, 34). Taken together, these findings represent the first demonstration that insulin is able to cause the translocation of fish GLUT4 in muscle cells. We previously described the translocation of okGLUT4 (a GLUT4-homolog in salmon) to the plasma membrane in response to insulin when expressed in 3T3-L1 adipocytes (4). Furthermore, this is the first report describing the insulin-regulated translocation of endogenous GLUT4 in fish cells. Therefore, fish GLUT4, like mammalian GLUT4, is regulated by insulin in terms of its translocation to the plasma membrane.

Endocytosis and recycling of btGLUT4

Although btGLUT4*myc*, as rat-GLUT4*myc*, was recruited to the plasma membrane in response to insulin in L6 cells, the steady-state level of btGLUT4*myc* at the cell surface under basal conditions was higher than that of rat-GLUT4*myc*. A similar observation was reported by Capilla *et al.* (4) in 3T3-L1 adipocytes transiently expressing okGLUT4, which also showed higher levels of transporter at the plasma membrane in the basal state than those expressing rat-GLUT4. Therefore, given the difference between btGLUT4 and rat-GLUT4 in protein motifs known to be important for GLUT4 trafficking, we hypothesized that the higher steady-state level of btGLUT4*myc* at the plasma membrane could be the result of different traffic mechanisms between fish and mammalian GLUT4. In mammalian muscle and adipose cells, GLUT4 is known to be continuously cycling between the plasma membrane and intracellular compartments (35). Thus, the amount of GLUT4 localized at the cell surface is a dynamic pool that depends on its exocytosis to the plasma membrane and its internalization to intracellular vesicles (36). Our results support the hypothesis that both transporters have a similar internalization rate, although btGLUT4*myc* reaches the plasma membrane (*i.e.* externalizes) more quickly than its mammalian counterpart. Therefore, because btGLUT4*myc* endocytosis does not differ from that of rat-GLUT4*myc*, the higher percentage of btGLUT4*myc* at the cell surface under basal conditions may only be explained by a faster recycling of the transporter to the plasma membrane.

Subcellular distribution of btGLUT4

After biosynthesis, GLUT4 is targeted from the trans-Golgi network (TGN) to specific membrane compartments that are insulin-responsive and referred to as the GLUT4 storage compartment (GSC) (37). Thus, these results suggest that a fraction of btGLUT4 could exit the exocytic route from the TGN to the GSC and instead follow directly from the TGN to the plasma membrane, like GLUT1 (37). Our observation that btGLUT4*myc* has a diffuse cytoplasmic distribution ecchoing than that of GLUT1 (38) would support this idea. However, it is also possible that btGLUT4 could reach the GSC but that it may not be efficiently retained and consequently travels to the plasma membrane. Interestingly, transient transfection of rat-GLUT4-HA in L6-btGLUT4*myc* myoblasts showed that in unstimulated cells btGLUT4*myc* does not completely colocalize with HA-tagged rat-GLUT4, exhibiting a more diffuse distribution throughout the cytoplasm. Conversely, rat-GLUT4*myc* showed a complete colocalization with transfected rat-GLUT4-HA in the perinuclear region. In support of our observations on L6-btGLUT4*myc* myoblasts, immunolocalization studies in primary brown trout muscle cells also demonstrated a diffuse distribution of btGLUT4 throughout the cytoplasm, although in fully differentiated myotubes, certain accumulation of btGLUT4 was observed in the perinuclear region. Therefore, our immunofluorescence experiments indicate that btGLUT4 has a different subcellular localization than rat-GLUT4 in muscle cells. Overall, our data suggest that btGLUT4 and rat-GLUT4 differ in their intracellular traffic mechanisms.

Possible mechanisms governing traffic of btGLUT4 and rat-GLUT4

It is tempting to speculate that the differences between btGLUT4 and rat-GLUT4 in terms of the sequence of particular protein motifs known to be important for GLUT4 traffic in mammalian cells could affect the interaction of btGLUT4 with regulatory proteins involved in the proper sorting and targeting of mammalian GLUT4. The dileucine motif at the carboxyl-cytoplasmic tail of mammalian GLUT4 has been described as crucial for its internalization from the plasma membrane as well as for its intracellular retention (19, 24, 39, 40). Interestingly, these two leucines at positions 489 and 490 are missing in the btGLUT4 sequence (5), arguing against an important role of this motif in GLUT4 internalization. Moreover, the dileucine motif has also been involved in GLUT4 targeting from the TGN to the GSC (21, 23). Furthermore, btGLUT4 also lacks two arginine residues located at positions -4 and -5 upstream from the dileucine signal that have been implicated along with the dileucine motif in

the intracellular sorting and endocytosis of mammalian GLUT4 (23). On the other hand, some authors have pointed to the importance of the amino-terminal FQQI motif in the intracellular localization of GLUT4 (20, 22, 41–43). In the btGLUT4 sequence, this motif is partially conserved (FQHL) but still contains the phenylalanine residue that appears to be essential for a proper GLUT4 sorting (42). Taking these sequence motif comparisons together with the fact that btGLUT4 presented the same internalization rate as rat-GLUT4, our data seem to support the notion that the FQQI motif is a major regulator of GLUT4 endocytosis. Therefore, btGLUT4 can be considered a natural mutant of GLUT4 that could assist in understanding the role of GLUT4 protein motifs in cellular traffic.

In addition to the structural GLUT4 motifs, several proteins have been shown to be important for mammalian GLUT4 traffic. Williams *et al.* (44) recently described that golgin-160, a protein localized to the Golgi cisternae, is required for the sorting of GLUT4 to the GSC, specifically for appropriate TGN sorting. As mentioned above, newly synthesized GLUT4 traffics from the TGN to GSC, and this sorting step is dependent on the GGA (Golgi localized, γ-ear containing, Arf binding protein) adaptor complex (37, 45). In addition, the Rab GTPase activating protein AS160 (Akt substrate of 160 kDa) contributes to the basal intracellular retention of GLUT4 (18, 46). This protein is associated with GLUT4 vesicles in the basal state and dissociates in response to insulin, allowing GLUT4 vesicles to travel to the plasma membrane. In myoblasts, this protein exerts its action via Rab proteins, particularly Rab8A and Rab14 (47). Neither golgin nor AS160 appears to interact directly with GLUT4. In contrast, TUG (tether, containing a UBX domain, for GLUT4) (48) interacts with the large cytosolic loop of GLUT4 forming a complex localized in the GSC, and upon insulin stimulation, this complex disassembles, allowing GLUT4 translocation to the plasma membrane. Recent studies have shown that disruption of TUG function leads to a redistribution of GLUT4 to the cell surface in the basal state (49). Other proteins such as α-actinin-4 and aldolase have been shown to link GLUT4 to the actin cytoskeleton (50, 51). In particular, α-actinin-4 coimmunoprecipitates with GLUT4 in L6 muscle cells in an insulin-dependent fashion (50). Therefore, the difference in traffic between fish and mammalian GLUT4 could be related to differences in their ability to interact with these and other proteins involved in the trafficking and intracellular sequestration of GLUT4. To date, some of these proteins have been identified in fish (Díaz, M., and J. Planas, unpublished observations); however, their role in regulating fish GLUT4 trafficking has not yet been elucidated. The effect of cytochalasin B and indinavir on glucose uptake in the L6 cell lines suggests that btGLUT4 is less sensitive to these transport inhibitors due to differences in amino acid sequence and/or conformation of the inhibitor binding site. Therefore, these results support our hypothesis that differences in btGLUT4 amino acid sequence may affect its interaction with proteins that bind mammalian GLUT4 and are involved in GLUT4 traffic.

Overall, our data indicate that insulin-stimulated translocation of btGLUT4 to the plasma membrane occurs in L6 and brown trout skeletal muscle cells in culture, resulting in an enhanced glucose transport activity in these cells. Increased basal exocytosis of btGLUT4 to the cell surface and diffuse localization of intracellular btGLUT4 suggest that the traffic of btGLUT4 differs from that of rat-GLUT4, probably due to differences in certain amino acid motifs that affect the sorting and/or intracellular retention of btGLUT4 in the perinuclear region. Further investigations will be needed to elucidate the sequence signals in GLUT4 that determine the difference in the traffic characteristics of btGLUT4 in comparison with that of rat-GLUT4. From an evolutionary perspective, it is interesting that, although the response of GLUT4 to insulin appears to be well conserved between fish and mammals, mammalian GLUT4 appears to have improved its intracellular retention, in addition to its affinity for glucose. Therefore, btGLUT4 could represent a useful tool with which to further our understanding of the cellular mechanisms regulating GLUT4 traffic in mammalian cells.

Acknowledgments

We thank Antonino Clemente (Piscifactoria de Bagà, Generalitat de Catalunya, Spain) for providing the brown trout and Dr. Marta Camps for her advice on immunofluorescence in primary myocytes. We also thank Dr. David E. James for the kind gift of cationic silica and his advice on plasma membrane preparation and Dr. Antonio Zorzano for his kind gift of GLUT1 Ab.

Received February 26, 2007. Accepted August 9, 2007.

Address all correspondence and requests for reprints to: Dr. Josep V. Planas, Departament de Fisiologia, Facultat de Biologia, Universitat de Barcelona, 08028 Barcelona, Spain. E-mail: jplanas@ub.edu.

This work was supported by Grants AGL2002-03987 and AGL2005-01230 (to J.V.P.) from Ministerio de Educación y Ciencia and a grant (to A.K.) from the Canadian Diabetes Association. M.D. was supported by a fellowship from the Departament d'Universitats, Recerca i Societat de la Informació (Generalitat de Catalunya). C.N.A. was supported by a doctoral award from the Canadian Diabetes Association.

Disclosure Statement: The authors of this manuscript have nothing to declare.

References

1. **Scheepers A, Joost HG, Schurmann A** 2004 The glucose transporter families SGLT and GLUT: molecular basis of normal and aberrant function. JPEN J Parenter Enteral Nutr 28:364–371
2. **Watson RT, Pessin JE** 2006 Bridging the GAP between insulin signaling and GLUT4 translocation. Trends Biochem Sci 31:215–222
3. **Ishiki M, Klip A** 2005 Minireview: recent developments in the regulation of glucose transporter-4 traffic: new signals, locations, and partners. Endocrinology 146:5071–5078
4. **Capilla E, Diaz M, Albalat A, Navarro I, Pessin JE, Keller K, Planas JV** 2004 Functional characterization of an insulin-responsive glucose transporter (GLUT4) from fish adipose tissue. Am J Physiol Endocrinol Metab 287:E348–357
5. **Planas JV, Capilla E, Gutierrez J** 2000 Molecular identification of a glucose transporter from fish muscle. FEBS Lett 481:266–270
6. **Blasco J, FernandezBorras J, Marimon I, Requena A** 1996 Plasma glucose kinetics and tissue uptake in brown trout *in vivo*: effect of an intravascular glucose load. J Comp Physiol [B] 165:534–541
7. **Moon TW** 2001 Glucose intolerance in teleost fish: fact or fiction? Comp Biochem Physiol B Biochem Mol Biol 129:243–249
8. **Capilla E, Diaz M, Gutierrez J, Planas JV** 2002 Physiological regulation of the expression of a GLUT4 homolog in fish skeletal muscle. Am J Physiol Endocrinol Metab 283:E44–E49
9. **Díaz M, Capilla E, Planas JV** 2007 Physiological regulation of glucose transporter (GLUT4) protein content in brown trout (*Salmo trutta*) skeletal muscle. J Exp Biol 210(Pt 13):2346–2351
10. **Rudich A, Klip A** 2003 Push/pull mechanisms of GLUT4 traffic in muscle cells. Acta Physiol Scand 178:297–308
11. **Ueyama A, Yaworsky KL, Wang Q, Ebina Y, Klip A** 1999 GLUT-4myc ectopic expression in L6 myoblasts generates a GLUT-4-specific pool conferring insulin sensitivity. Am J Physiol 277:E572–E578

12. **Niwa H, Yamamura K, Miyazaki J** 1991 Efficient selection for high-expression transfectants with a novel eukaryotic vector. Gene 108:193–199
13. **Castillo J, Le Bail PY, Paboeuf G, Navarro I, Weil C, Fauconneau B, Gutierrez J** 2002 IGF-I binding in primary culture of muscle cells of rainbow trout: changes during *in vitro* development. Am J Physiol Regul Integr Comp Physiol 283:R647–R652
14. **Fauconneau B, Paboeuf G** 2000 Effect of fasting and refeeding on *in vitro* muscle cell proliferation in rainbow trout (*Oncorhynchus mykiss*). Cell Tissue Res 301:459–463
15. **Wang Q, Khayat Z, Kishi K, Ebina Y, Klip A** 1998 GLUT4 translocation by insulin in intact muscle cells: detection by a fast and quantitative assay. FEBS Lett 427:193–197
16. **Huang C, Thirone AC, Huang X, Klip A** 2005 Differential contribution of insulin receptor substrates 1 versus 2 to insulin signaling and glucose uptake in l6 myotubes. J Biol Chem 280:19426–19435
17. **Chaney LK, Jacobson BS** 1983 Coating cells with colloidal silica for high yield isolation of plasma membrane sheets and identification of transmembrane proteins. J Biol Chem 258:10062–10072
18. **Larance M, Ramm G, Stockli J, van Dam EM, Winata S, Wasinger V, Simpson F, Graham M, Junutula JR, Guilhaus M, James DE** 2005 Characterization of the role of the Rab GTPase-activating protein AS160 in insulin-regulated GLUT4 trafficking. J Biol Chem 280:37803–37813
19. **Corvera S, Chawla A, Chakrabarti R, Joly M, Buxton J, Czech MP** 1994 A double leucine within the GLUT4 glucose transporter COOH-terminal domain functions as an endocytosis signal. J Cell Biol 126:979–989
20. **Garippa RJ, Judge TW, James DE, McGraw TE** 1994 The amino terminus of GLUT4 functions as an internalization motif but not an intracellular retention signal when substituted for the transferrin receptor cytoplasmic domain. J Cell Biol 124:705–715
21. **Martinez-Arca S, Lalioti VS, Sandoval IV** 2000 Intracellular targeting and retention of the glucose transporter GLUT4 by the perinuclear storage compartment involves distinct carboxyl-tail motifs. J Cell Sci 113(Pt 10):1705–1715
22. **Piper RC, Tai C, Kulesza P, Pang S, Warnock D, Baenziger J, Slot JW, Geuze HJ, Puri C, James DE** 1993 GLUT-4 NH2 terminus contains a phenylalanine-based targeting motif that regulates intracellular sequestration. J Cell Biol 121:1221–1232
23. **Sandoval IV, Martinez-Arca S, Valdueza J, Palacios S, Holman GD** 2000 Distinct reading of different structural determinants modulates the dileucine-mediated transport steps of the lysosomal membrane protein LIMPII and the insulin-sensitive glucose transporter GLUT4. J Biol Chem 275:39874–39885
24. **Verhey KJ, Birnbaum MJ** 1994 A Leu-Leu sequence is essential for COOH-terminal targeting signal of GLUT4 glucose transporter in fibroblasts. J Biol Chem 269:2353–2356
25. **Beguinot F, Kahn CR, Moses AC, Smith RJ** 1986 The development of insulin receptors and responsiveness is an early marker of differentiation in the muscle cell line L6. Endocrinology 118:446–455
26. **Ramlal T, Sarabia V, Bilan PJ, Klip A** 1988 Insulin-mediated translocation of glucose transporters from intracellular membranes to plasma membranes: sole mechanism of stimulation of glucose transport in L6 muscle cells. Biochem Biophys Res Commun 157:1329–1335
27. **Walker PS, Ramlal T, Donovan JA, Doering TP, Sandra A, Klip A, Pessin JE** 1989 Insulin and glucose-dependent regulation of the glucose transport system in the rat L6 skeletal muscle cell line. J Biol Chem 264:6587–6595
28. **Antonescu CN, Huang C, Niu W, Liu Z, Eyers PA, Heidenreich KA, Bilan PJ, Klip A** 2005 Reduction of insulin-stimulated glucose uptake in L6 myotubes by the protein kinase inhibitor SB203580 is independent of p38MAPK activity. Endocrinology 146:3773–3781
29. **Niu W, Huang C, Nawaz Z, Levy M, Somwar R, Li D, Bilan PJ, Klip A** 2003 Maturation of the regulation of GLUT4 activity by p38 MAPK during L6 cell myogenesis. J Biol Chem 278:17953–17962
30. **Castillo J, Codina M, Martinez ML, Navarro I, Gutierrez J** 2004 Metabolic and mitogenic effects of IGF-I and insulin on muscle cells of rainbow trout. Am J Physiol Regul Integr Comp Physiol 286:R935–R941
31. **Duclos MJ, Chevalier B, Le Marchand-Brustel Y, Tanti JF, Goddard C, Simon J** 1993 Insulin-like growth factor-I-stimulated glucose transport in myotubes derived from chicken muscle satellite cells. J Endocrinol 137:465–472
32. **Roe JA, Baba AS, Harper JM, Buttery PJ** 1995 Effects of growth factors and gut regulatory peptides on nutrient uptake in ovine muscle cell cultures. Comp Biochem Physiol A Physiol 110:107–114
33. **Al-Khalili L, Chibalin AV, Kannisto K, Zhang BB, Permert J, Holman GD, Ehrenborg E, Ding VD, Zierath JR, Krook A** 2003 Insulin action in cultured human skeletal muscle cells during differentiation: assessment of cell surface GLUT4 and GLUT1 content. Cell Mol Life Sci 60:991–998
34. **Sarabia V, Lam L, Burdett E, Leiter LA, Klip A** 1992 Glucose transport in human skeletal muscle cells in culture. Stimulation by insulin and metformin. J Clin Invest 90:1386–1395
35. **Dugani CB, Klip A** 2005 Glucose transporter 4: cycling, compartments and controversies. EMBO Rep 6:1137–1142
36. **Karylowski O, Zeigerer A, Cohen A, McGraw TE** 2004 GLUT4 is retained by an intracellular cycle of vesicle formation and fusion with endosomes. Mol Biol Cell 15:870–882
37. **Watson RT, Khan AH, Furukawa M, Hou JC, Li L, Kanzaki M, Okada S, Kandror KV, Pessin JE** 2004 Entry of newly synthesized GLUT4 into the insulin-responsive storage compartment is GGA dependent. EMBO J 23:2059–2070
38. **Kaliman P, Vinals F, Testar X, Palacin M, Zorzano A** 1995 Disruption of GLUT1 glucose carrier trafficking in L6E9 and Sol8 myoblasts by the phosphatidylinositol 3-kinase inhibitor wortmannin. Biochem J 312(Pt 2):471–477
39. **Haney PM, Levy MA, Strube MS, Mueckler M** 1995 Insulin-sensitive targeting of the GLUT4 glucose transporter in L6 myoblasts is conferred by its COOH-terminal cytoplasmic tail. J Cell Biol 129:641–658
40. **Verhey KJ, Yeh JI, Birnbaum MJ** 1995 Distinct signals in the GLUT4 glucose transporter for internalization and for targeting to an insulin-responsive compartment. J Cell Biol 130:1071–1079
41. **Al-Hasani H, Kunamneni RK, Dawson K, Hinck CS, Muller-Wieland D, Cushman SW** 2002 Roles of the N- and C-termini of GLUT4 in endocytosis. J Cell Sci 115:131–140
42. **Khan AH, Capilla E, Hou JC, Watson RT, Smith JR, Pessin JE** 2004 Entry of newly synthesized GLUT4 into the insulin-responsive storage compartment is dependent upon both the amino terminus and the large cytoplasmic loop. J Biol Chem 279:37505–37511
43. **Marsh BJ, Alm RA, McIntosh SR, James DE** 1995 Molecular regulation of GLUT-4 targeting in 3T3–L1 adipocytes. J Cell Biol 130:1081–1091
44. **Williams D, Hicks SW, Machamer CE, Pessin JE** 2006 Golgin-160 is required for the Golgi membrane sorting of the insulin-responsive glucose transporter GLUT4 in adipocytes. Mol Biol Cell 17:5346–5355
45. **Li LV, Kandror KV** 2005 Golgi-localized, γ-ear-containing, Arf-binding protein adaptors mediate insulin-responsive trafficking of glucose transporter 4 in 3T3–L1 adipocytes. Mol Endocrinol 19:2145–2153
46. **Eguez L, Lee A, Chavez JA, Miinea CP, Kane S, Lienhard GE, McGraw TE** 2005 Full intracellular retention of GLUT4 requires AS160 Rab GTPase activating protein. Cell Metab 2:263–272
47. **Ishikura S, Bilan PJ, Klip A** 2007 Rabs 8A and 14 are targets of the insulin-regulated Rab-GAP AS160 regulating GLUT4 traffic in muscle cells. Biochem Biophys Res Commun 353:1074–1079
48. **Bogan JS, Hendon N, McKee AE, Tsao TS, Lodish HF** 2003 Functional cloning of TUG as a regulator of GLUT4 glucose transporter trafficking. Nature 425:727–733
49. **Yu C, Cresswell J, Loffler MG, Bogan JS** 2007 The glucose transporter 4-regulating protein TUG is essential for highly insulin-responsive glucose uptake in 3T3–L1 adipocytes. J Biol Chem 282:7710–7722
50. **Foster LJ, Rudich A, Talior I, Patel N, Huang X, Furtado LM, Bilan PJ, Mann M, Klip A** 2006 Insulin-dependent interactions of proteins with GLUT4 revealed through stable isotope labeling by amino acids in cell culture (SILAC). J Proteome Res 5:64–75
51. **Kao AW, Noda Y, Johnson JH, Pessin JE, Saltiel AR** 1999 Aldolase mediates the association of F-actin with the insulin-responsive glucose transporter GLUT4. J Biol Chem 274:17742–17747

***Endocrinology* is published monthly by The Endocrine Society (http://www.endo-society.org), the foremost professional society serving the endocrine community.**